

Columnar Structure in Bulk Heterojunction in Solution-Processable Three-Layered p-i-n Organic Photovoltaic Devices Using Tetrabenzoporphyrin Precursor and Silylmethyl[60]fullerene

Yutaka Matsuo,^{*,†,‡} Yoshiharu Sato,^{*,†} Takaaki Niinomi,[†] Iwao Soga,[†] Hideyuki Tanaka,[†] and Eiichi Nakamura^{*,†,‡}

Nakamura Functional Carbon Cluster Project, ERATO, Japan Science and Technology Agency, Hongo, Bunkyo-ku, Tokyo 113-0033, Japan, and Department of Chemistry, The University of Tokyo, Hongo, Bunkyo-ku, Tokyo 113-0033, Japan

Received June 15, 2009; E-mail: matsuo@chem.s.u-tokyo.ac.jp; ysato@chem.s.u-tokyo.ac.jp; nakamura@chem.s.u-tokyo.ac.jp

Organic photovoltaic (OPV) devices based on the single active layer bulk heterojunction (BHJ) concept¹ offer a realistic possibility of low-cost photoenergy conversion systems.² However, there are two issues that need to be resolved: One is the rather narrow repertoire of materials,³ especially acceptor materials, and the other is the lack of precise structural information on the BHJ layer, the heart of the device,⁴ where photoexcitation and charge separation occur.⁵ The presumed structures of an ideal BHJ are the following: the BHJ should consist of interdigitated donor and acceptor molecular aggregates,⁶ and the aggregates should be comparable in size to the exciton diffusion length.⁷ We report here that a new solution-processable, small-molecule based fabrication process allows us to obtain a three-layered p-i-n structure⁸ in which the

i-layer possesses a clearly defined interdigitated structure formed by spontaneous crystalline phase separation during thermal processing. This device shows a power-conversion efficiency (PCE) of 5.2%, a value that ranks among the best of those reported for solution-processed small-molecule based OPV cells.⁹

The present work features new types of small-molecule OPV materials, a soluble CP molecule (1,4:8,11:15,18:22,25-tetraethano-29H,31H-tetrabenzob[*b,g,l,q*]porphyrin, Figure 1a) that is thermally

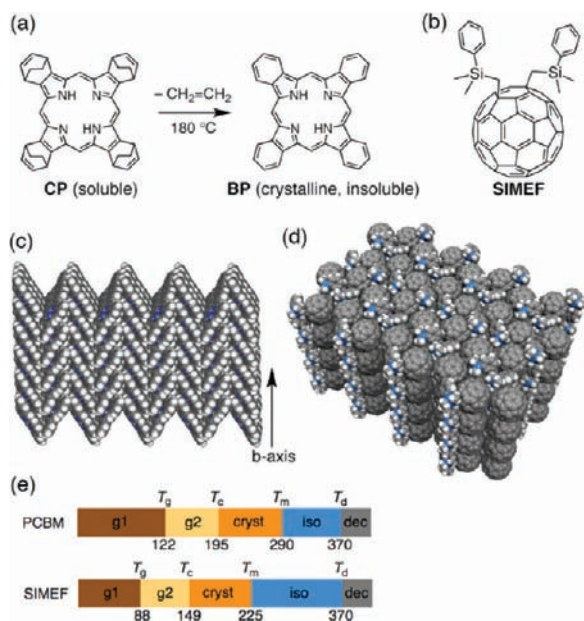


Figure 1. Donor and acceptor materials for three-layered OPV devices. (a) Thermal retro-Diels–Alder conversion of CP (donor precursor) to BP (donor) at 180 °C. (b) SIMEF (acceptor). (c) π – π Stacking of BP in crystals and the crystal *b*-axis along which the crystal grows. (d) Near-hexagonal crystal packing of SIMEF that crystallizes without solvent inclusion. (e) Thermal behavior of SIMEF and PCBM. The letter *g* stands for glass phase, *cryst* for crystalline, *iso* for isotropic, and *dec* for decomposition (unit = °C).

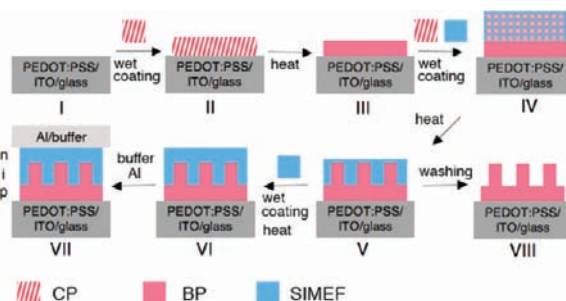


Figure 2. Solution-processable p-i-n three-layered organic photovoltaic devices.

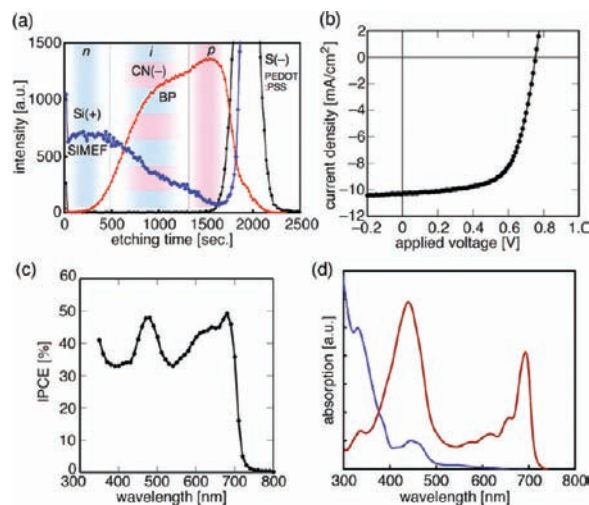


Figure 3. Structural analysis of VI and performance of the devices. (a) TOF-SIMS data for the BP/PCBM/SIMEF/SIMEF p-i-n structure on a PEDOT:PSS/silicon substrate. SIMEF, BP, and PEDOT:PSS were monitored by Si⁺, CN⁻, and S⁻ ions, respectively. Color coding corresponds to the color used for VI in Figure 2. (b) The *J*–*V* curve for the OPV device that shows a 5.0% PCE ($V_{OC} = 0.75$ V; $J_{SC} = 10.3$ mA/cm²; FF = 0.65). (c) IPCE profile of the 5.0%-device with a maximum external quantum yield at 460 and 670 nm. (d) Absorption spectra of BP (red) and SIMEF (blue), which agree with the IPCE profile.

[†] Japan Science and Technology Agency.

[‡] The University of Tokyo.

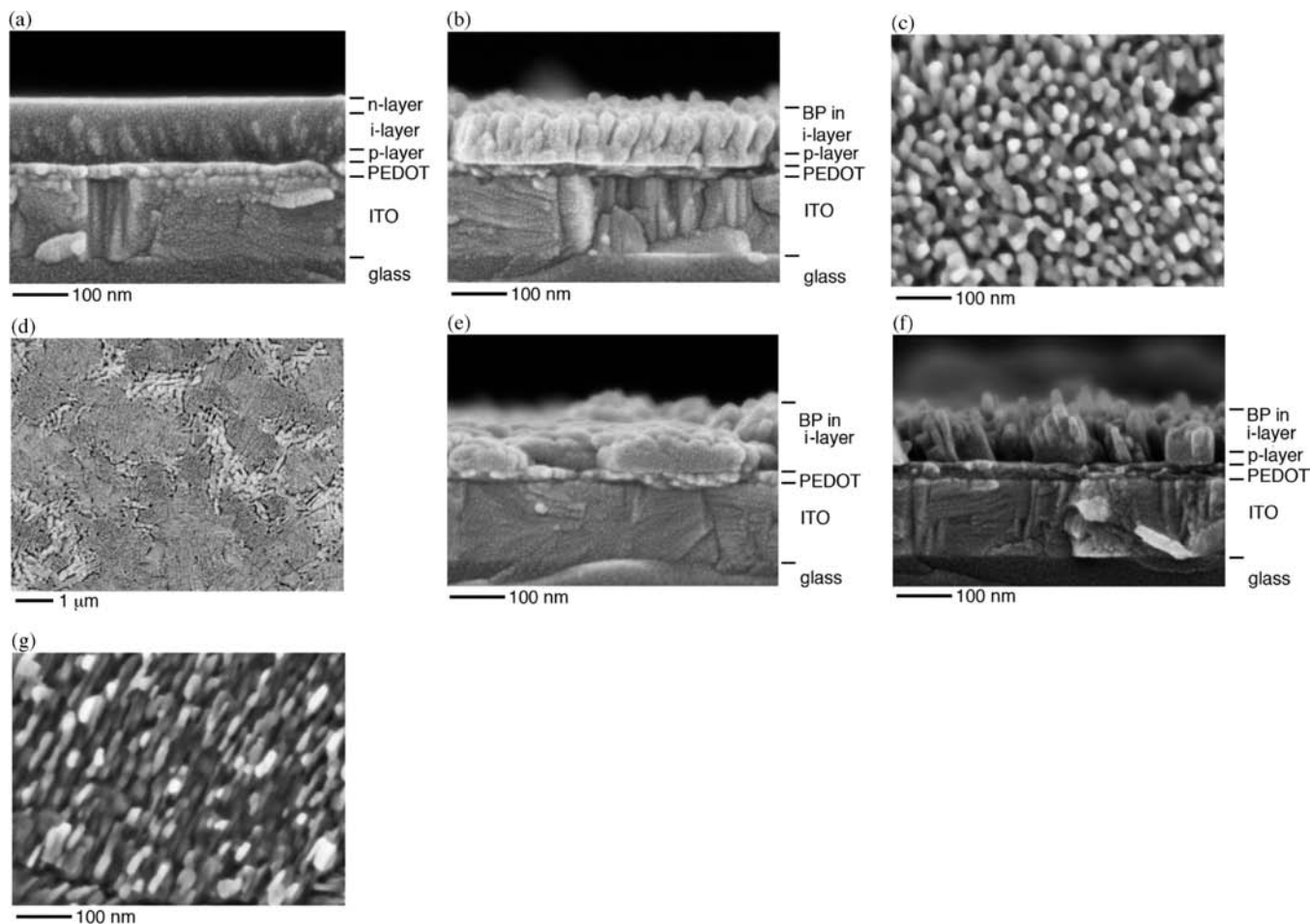


Figure 4. SEM images of the p-i-n structure VI made from BP and SIMEF (glass/ITO/PEDOT:PSS/BP/BP:SIMEF/SIMEF), and its toluene-washed structure VIII, as well as a corresponding device using PCBM (f, g) (glass/ITO/PEDOT:PSS/BP/BP:PCBM/PCBM). (a) Side view of the p-i-n structure (VI). (b) Side view of the column/canyon region of the p-i structure in VIII. (c) Top view of the column/canyon region of VIII. (d) A wide-area image of the top view of VIII. The dominant dark gray area (ca. 60%) is the column/canyon region, and the light gray area contains much larger BP crystals. (e) Side view of the larger BP crystal area. (f) Side view of the toluene-washed BP:PCBM device VIII, where rectangular BP crystals grow irregularly. (g) Top view of Figure 4f that shows the growth of rectangular BP crystals, which is very different from that shown in Figure 4c. Larger images are provided in the Supporting Information.

converted to a highly insoluble, crystalline tetrabenzoporphyrin (BP) donor (Figure 1a, and its crystal packing in Figure 1c),^{10,11} and a new fullerene acceptor, bis(dimethylphenylsilylmethyl)[60]fullerenes (SIMEF, Figure 1b), which undergoes thermal transition from amorphous to crystal at 149 °C (Figure 1d,e).¹² SIMEF has a LUMO level (−3.74 eV) that is ca. 0.1 eV higher than that in the commonly used PCBM (phenyl C61-butyl acid methyl ester)¹³ acceptor and a much lower crystallization temperature (Figure 1e).

The fabrication method of our solution-processed device is illustrated in Figure 2, in which the CP-to-BP thermal conversion after spin coating plays a crucial role in the creation of a defined BHJ structure in the i-layer (VII). Note that BP crystals are virtually insoluble in organic solvents and cannot be spin-coated. In addition, BP is immiscible with SIMEF and PCBM.

A solution of the donor precursor CP (hatched red) in chloroform/chlorobenzene is first spin-coated on the glass/ITO/PEDOT:PSS electrode (I) to form II and is thermally converted to the donor BP (red) at 180 °C to form a donor p-layer (III). In the second step, a homogeneous mixture (a typical weight ratio of 3:7) of CP and an acceptor SIMEF (blue) in chloroform/chlorobenzene¹⁴ is spin-coated (IV), and CP is converted in situ to BP (red) at 180 °C to form an interdigitated i-layer (V). The choice of 180 °C is crucial to the swift conversion of CP to BP in the presence of SIMEF, which is

crystalline at this temperature. Subsequent spin coating of SIMEF in toluene on V and heating at 65 or 180 °C (to crystallize SIMEF) furnishes the p-i-n structure (VI). A buffer material (phenanthroline derivatives: bathocuproine (BCP) or 2,9-bis(naphthalen-2-yl)-4,7-diphenyl-1,10-phenanthroline (NBphen)) and an aluminum electrode are coated in a vacuum to complete the device for testing (VII). Removal of the acceptor by washing V or VI with toluene leaves behind a column/canyon structure (VIII), which can be studied by SEM.

To examine whether each layer was formed properly, we first analyzed the structure corresponding to VI (fabricated on silicon; Figure 3a) by time-of-flight secondary ion mass spectrometry (TOF-SIMS). From the time data (*x*-axis) that are related to the depth from the surface, we can determine an approximate relative thicknesses of 1.5:5:1.5:2 for the n-, i-, p-, and PEDOT:PSS layers.

The SEM analysis (Figure 4) of structures VI and VIII gave us visual evidence of the desired p-i-n structure and revealed a columnar BP crystal formation in the i-layer. Thus, Figure 4a shows a side view of VI, in which one can identify n-, i-, p-, and PEDOT:PSS layers (total thickness ca. 110 nm). The depth profile agrees with the TOF-SIMS depth data.

The desired interdigitated BHJ in the i-layer that is vaguely visible in Figure 4a can be seen more clearly after removal of

SIMEF (VIII). The round columns stand almost vertically on the ca. 20-nm-thick p-layer (Figure 4b). Figure 4c illustrates an intriguing top view of the column/canyon structure. The wide-area SEM image (Figure 4d) showed that the column/canyon area (fine grain, dark gray) accounts for the dominant area, and the rest consists of a less uniform, larger grain area (Figure 4e), in which a large chunk of BP crystals grows directly on the PEDOT:PSS layer. Separate experiments indicated that devices without the p-layer show less than 1% PCE.

The average size of the columns in Figure 4b, c is 65 nm ($\sigma = 13$ nm) in height and 26 nm ($\sigma = 7$ nm) in diameter (average of ca. 120 columns). Each column is estimated to contain 30 000–100 000 BP molecules, based upon the unit cell parameter of the BP crystal packing structure (Figure 1c).¹⁵ Since this is comparable to the exciton diffusion length of common organic semiconducting materials (10–30 nm),¹⁶ the columns are a suitable size for charge separation and carrier transport.

We used PCBM in place of SIMEF, fabricated the device under the same conditions, and found that the BP crystal morphology in the i-layer is far less uniform in size than that in the SIMEF device (Figure 4f,g). In addition, the BP crystals are rectangular (a usual bulk morphology of BP crystals) rather than round columnar. We ascribe this difference to the crystallization temperatures of SIMEF (149 °C) and PCBM (195 °C). Thus, BP crystal formation at 180 °C in the SIMEF device occurs in the matrix of SIMEF crystals, while it occurs in amorphous PCBM in the PCBM device (Figures S4 and S5).

The BP/SIMEF devices exhibit respectable performance. The glass/ITO/PEDOT:PSS/BP/PCBM/SIMEF/SIMEF/BCP/Al cell that was heated at 65 °C after n-layer formation showed 4.1% PCE (open circuit voltage, $V_{OC} = 0.76$ V; short circuit current density, $J_{SC} = 9.1$ mA/cm²; fill factor, FF = 0.59).¹⁷ The same device heated at 180 °C after the n-layer fabrication reproducibly showed 4.5% ($V_{OC} = 0.76$ V; $J_{SC} = 9.7$ mA/cm²; FF = 0.62). The improvement of J_{SC} and FF suggests that the crystallization of SIMEF in the n-layer at ca. 150 °C contributed to this improvement.¹² Further optimization with the use of NBphen buffer afforded PCE = 4.8–5.2% (parameters for the 5.2%-device: $V_{OC} = 0.75$ V; $J_{SC} = 10.5$ mA/cm²; FF = 0.65; Figure 3b–d). The device lacking the i-layer (glass/ITO/PEDOT:PSS/BP/SIMEF/BCP/Al) showed only 2.3% PCE.

When we used PCBM in place of SIMEF, the PCE decreased to 2.0% owing to lower V_{OC} (0.55 V), J_{SC} (7.0 mA/cm²), and FF (0.51). We ascribe this decrease to the undesirable i-layer morphology (vide supra) and to the lower LUMO level of PCBM (by ca. 0.1 V).^{12,18}

In summary, a new solution-processable fabrication afforded p-i-n OPV devices composed of BP and SIMEF. The device showed a respectable performance of 5.2% PCE. The structure of the interdigitated BHJ structure of the charge-separating i-layer has been clearly imaged with SEM. Thus, the SEM images revealed a nanoscale column/canyon BHJ morphology in the dominant area of the i-layer. The controllable BHJ structure and the respectable performance of the present prototype attest to the need for further examination of small molecules and new device structures for the production of efficient organic solar cells.

Acknowledgment. We thank the Mitsubishi Chemical Group Science and Technology Research Center, Inc. for sharing their insights and for provision of CP and analytical data. We also thank Dr. Masaki Takashima for the SEM images and Dr. Keiko Matsuo for helpful experimental data. This research was partially supported by KAKENHI (18105004).

Supporting Information Available: Method for fabrication of the OPV devices and SEM images. This material is available free of charge via the Internet at <http://pubs.acs.org>.

References

- (1) (a) *Organic Photovoltaics. Concept and Realization*; Brabec, C., Dyakonov, V., Parisi, J., Saritiftci, N. S., Eds.; Springer Verlag: Berlin, 2003. (b) Yu, G.; Gao, J.; Hummelen, J. C.; Wudl, F.; Heeger, A. J. *Science* **1995**, *270*, 1789–1791.
- (2) (a) Kim, J. Y.; Kim, S. H.; Lee, H.-H.; Lee, K.; Ma, W.; Gong, X.; Heeger, A. J. *Adv. Mater.* **2006**, *18*, 572–576. (b) Kim, J. Y.; Lee, K.; Coates, N. E.; Moses, D.; Nguyen, T.-Q.; Dante, M.; Heeger, A. J. *Science* **2007**, *317*, 222–225.
- (3) (a) Lloyd, M. T.; Mayer, A. C.; Tayi, A. S.; Bowen, A. M.; Kasen, T. G.; Herman, D. J.; Mourey, D. A.; Anthony, J. E.; Malliaras, G. G. *Org. Electron.* **2006**, *7*, 243–248. (b) Ma, C. Q.; Mena-Osteritz, E.; Debaerdtmaeker, T.; Wienk, M. M.; Janssen, R. A. J.; Bäuerle, P. *Angew. Chem., Int. Ed.* **2007**, *46*, 1679–1683.
- (4) (a) Hoppe, H.; Niggemann, M.; Winder, C.; Kraut, J.; Hiesgen, R.; Hinsch, A.; Meissner, D.; Sariciftci, N. S. *Adv. Funct. Mater.* **2004**, *14*, 1005–1011. (b) Hoppe, H.; Sariciftci, N. S. *J. Mater. Chem.* **2006**, *16*, 45–61. (c) Moon, J. S.; Lee, J. K.; Cho, S.; Byun, J.; Heeger, A. J. *Nano Lett.* **2009**, *9*, 230–234.
- (5) Sariciftci, N. S.; Smilowitz, L.; Heeger, A. J.; Wudl, F. *Science* **1992**, *258*, 1474–1476.
- (6) (a) Xue, J.; Rand, B. P.; Uchida, S.; Forrest, S. R. *Adv. Mater.* **2005**, *17*, 66–71. (b) Hiramoto, M.; Yamaga, T.; Danno, M.; Suemori, K.; Matsumura, Y.; Yokoyama, M. *Appl. Phys. Lett.* **2006**, *88*, 213105. (c) Taima, T.; Toyoshima, S.; Hara, K.; Saito, K.; Yase, K. *Jpn. J. Appl. Phys.* **2006**, *45*, L217–L219. (d) Schmidt-Mende, L.; Fechtenkötter, A.; Müllen, K.; Moons, E.; Friend, R. H.; MacKenzie, J. D. *Science* **2001**, *293*, 1119–1122. (e) Li, G.; Shrotriya, V.; Huang, J.; Yao, Y.; Moriarty, T.; Emery, K.; Yang, Y. *Nat. Mater.* **2005**, *4*, 864–868. (f) Kim, Y.; Cook, S.; Tuladhar, S. M.; Choulis, S. A.; Nelson, J.; Durrant, J. R.; Bradley, D. D. C.; Giles, M.; McCulloch, I.; Ha, C.-S.; Ree, M. *Nat. Mater.* **2006**, *5*, 197. (g) Kim, K.; Liu, J.; Namboothiry, M. A. G.; Carroll, D. L. *Appl. Phys. Lett.* **2007**, *90*, 163511. (h) Kennedy, R. D.; Ayzner, A. L.; Wanger, D. D.; Day, C. T.; Halim, M.; Khan, S. I.; Tolbert, S. H.; Schwartz, B. J.; Rubin, Y. *J. Am. Chem. Soc.* **2008**, *130*, 17290–17292. (i) Niinomi, T.; Matsuo, Y.; Hashiguchi, M.; Sato, Y.; Nakamura, E. *J. Mater. Chem.* **2009**, *19*, 5804–5811.
- (7) Peumans, P.; Yakimov, A.; Forrest, S. R. *J. Appl. Phys.* **2003**, *93*, 3693–3723.
- (8) (a) Gebeyehu, D.; Pfeiffer, M.; Maennig, B.; Drechsel, J.; Werner, A.; Leo, K. *Thin Solid Films* **2004**, *451/452*, 29–32. (b) Suemori, K.; Miyata, T.; Yokoyama, M.; Hiramoto, M. *Appl. Phys. Lett.* **2005**, *86*, 063509.
- (9) Tamayo, A. B.; Dang, X.-D.; Walker, B.; Seo, J.; Kent, T.; Nguyen, T.-Q. *Appl. Phys. Lett.* **2009**, *94*, 103301.
- (10) Ito, S.; Murashima, T.; Uno, H.; Ono, N. *Chem. Commun.* **1998**, 1661–1662.
- (11) Aramaki, S.; Sakai, Y.; Ono, N. *Appl. Phys. Lett.* **2004**, *84*, 2085–2087.
- (12) Matsuo, Y.; Iwashita, A.; Abe, Y.; Li, C.-Z.; Matsuo, K.; Hashiguchi, M.; Nakamura, E. *J. Am. Chem. Soc.* **2008**, *130*, 15429–15436.
- (13) Hummelen, J. C.; Knight, B. W.; LePeq, F.; Wudl, F. *J. Org. Chem.* **1995**, *60*, 532–538.
- (14) CP and SIMEF are monomeric in this solution (dynamic light scattering).
- (15) Aramaki, S.; Mizuguchi, J. *Acta Crystallogr., Sect. E* **2003**, *59*, o1556–o1558.
- (16) Peumans, P.; Yakimov, A.; Forrest, S. R. *J. Appl. Phys.* **2003**, *93*, 3693–3723.
- (17) The i-layer thickness has been optimized. Thicker and thinner devices tend to give lower J_{SC} .
- (18) (a) Kooistra, F. B.; Knol, J.; Kastenbergh, F.; Popescu, L. M.; Verhees, W. J. H.; Kroon, J. M.; Hummelen, J. C. *Org. Lett.* **2007**, *9*, 551–554. (b) Lenes, M.; Wetzelaer, G.-J. A. H.; Kooistra, F. B.; Veenstra, S. C.; Hummelen, J. C.; Blom, P. W. M. *Adv. Mater.* **2008**, *20*, 2116–2119.

JA9048702